




Research Article

Estimating Abundance of an Unmarked, Low-Density Species using Cameras

KENNETH E. LOONAM ¹, *Montana Cooperative Wildlife Research Unit, Wildlife Biology Program, University of Montana, 205 Natural Sciences Building, Missoula, MT 59812, USA*

DAVID E. AUSBAND,² *Idaho Department of Fish and Game, 2885 Kathleen Avenue, Coeur d'Alene, ID 83815, USA*

PAUL M. LUKACS, *Wildlife Biology Program, Department of Ecosystem and Conservation Sciences, W.A. Franke College of Forestry and Conservation, University of Montana, 32 Campus Drive, Missoula, MT 59812*

MICHAEL S. MITCHELL, *U.S. Geological Survey, Montana Cooperative Wildlife Research Unit, Wildlife Biology Program, University of Montana, 205 Natural Sciences Building, Missoula, MT 59812, USA*

HUGH S. ROBINSON, *Panthera and Wildlife Biology Program, W.A. Franke College of Forestry and Conservation, University of Montana, 205 Natural Sciences Building, Missoula, MT 59812, USA*

ABSTRACT Estimating abundance of wildlife populations can be challenging and costly, especially for species that are difficult to detect and that live at low densities, such as cougars (*Puma concolor*). Remote, motion-sensitive cameras are a relatively efficient monitoring tool, but most abundance estimation techniques using remote cameras rely on some or all of the population being uniquely identifiable. Recently developed methods estimate abundance from encounter rates with remote cameras and do not require identifiable individuals. We used 2 methods, the time-to-event and space-to-event models, to estimate the density of 2 cougar populations in Idaho, USA, over 3 winters from 2016–2019. We concurrently estimated cougar density using the random encounter model (REM), an existing camera-based method for unmarked populations, and genetic spatial capture recapture (SCR), an established method for monitoring cougar populations. In surveys for which we successfully estimated density using the SCR model, the time-to-event estimates were more precise and showed comparable variation between survey years. The space-to-event estimates were less precise than the SCR estimates and were more variable between survey years. Compared to REM, time-to-event was more precise and consistent, and space-to-event was less precise and consistent. Low sample sizes made the space-to-event and SCR models inconsistent from survey to survey, and non-random camera placement may have biased both of the camera-based estimators high. We show that camera-based estimators can perform comparably to existing methods for estimating abundance in unmarked species that live at low densities. With the time- and space-to-event models, managers could use remote cameras to monitor populations of multiple species at broader spatial and temporal scales than existing methods allow. © 2020 The Wildlife Society.

KEY WORDS abundance, camera, cougar, density, monitoring, mountain lion, noninvasive, *Puma concolor*, time-to-event, unmarked.

Camera surveys are a common method for monitoring elusive species and species that live at low densities (O'Connell et al. 2011). When individuals in a population can be uniquely identified from photographs, camera data can be used to estimate abundance through capture-recapture and spatial capture-recapture (SCR; Karanth 1995, Karanth and Nichols 1998, Royle et al. 2009). Most species do not consist of uniquely identifiable individuals, so estimating abundance requires methods for unmarked populations. Quantifying the relationship between photographic rate and density (Carbone et al. 2001, Rowcliffe et al. 2008, Moeller et al. 2018) can be

effective at estimating the abundance of elusive species that live at low densities and do not have unique marks (Cusack et al. 2015), but as yet none of these methods have been widely adopted.

The time-to-event and space-to-event models use time-to-event analysis to estimate density from the encounter rate between animals and cameras (Moeller et al. 2018). At higher densities, encounter rate is higher, reducing the time between photographic events. The time-to-event model uses repeated measures of the time until an animal appears on camera and an estimate of animal movement speed to estimate density using

$$\text{TTE} \sim \text{Exp}(\lambda), \quad (1)$$

where TTE is the observed distribution of the number of periods until an animal appears on camera and λ is density

Received: 18 February 2020; Accepted: 4 August 2020

¹E-mail: kenneth.loonam@umontana.edu

²Current affiliation: U.S. Geological Survey, Idaho Cooperative Fish and Wildlife Research Unit, University of Idaho, 875 Perimeter Drive MS 1141, Moscow, ID 83844, USA

in animals per viewshed (i.e., the area photographed). A period is defined as the time an animal moving at the mean movement rate of the population (including rest time) would spend in a camera's viewshed. For example, for a population that moves at 10 m/minute and viewsheds are 10 m wide, a period would be 1 minute. If the movement speed changed to 5 m/minute, a period would be 2 minutes. If an animal appears during the first period, TTE is 1; if an animal does not appear until the third period, TTE is 3. For λ , the number of animals per viewshed, to reflect the density of animals in the study area, cameras should be placed randomly with respect to animal movement. The space-to-event model functions similarly but measures the amount of space sampled until an animal appears on camera rather than measuring the amount of time until an animal appears. The space-to-event model estimates density using

$$\text{STE} \sim \text{Exp}(\lambda), \quad (2)$$

where STE is the number of camera viewsheds randomly sampled at a single point in time before an animal is observed. In other words, at each time step, cameras are selected randomly, without replacement, until a camera with an animal in view is selected. The STE for that time step is recorded as the number of cameras sampled. The space-to-event model still requires cameras to be placed randomly with respect to animal movement, but by sampling across cameras at a given time and allowing the animals to move between temporal samples, the space-to-event model eliminates the need for an estimate of animal movement speed. The space-to-event model can also reduce the reliance on motion trigger detections by allowing cameras to be set to take a single picture on each occasion. Like the time-to-event model, the space-to-event model measures the effort required to observe a single animal (measured in area sampled) to estimate density. This separates the space-to-event model from distance sampling with motion-sensitive cameras, which relies on counts of animals at varying distances from the camera to estimate detection probabilities (Howe et al. 2017, Gilbert et al. 2020).

Evaluating the efficacy of a new abundance estimator requires a point of comparison. Ideally, estimates are compared to truth by surveying a population of known size (Rowcliffe et al. 2008), but populations of known size are rarely available and often represent idealized conditions. When populations of known size are not available, estimates from the new method can be compared to reasonable expectations based on prior knowledge (Karanth 1995) or to concurrent estimates of the same population using alternative, established methods (Efford 2004).

Cougars (*Puma concolor*) are a challenging species to monitor because they are elusive, naturally unmarked, and live at low densities. Historically cougar populations were quantified using a census technique in which researchers attempted to collar or mark all resident animals in a study area (Hornocker 1969, Seidensticker et al. 1973). More recently cougar populations have been quantified using genetic SCR (Brochers and Efford 2008, Royle and

Young 2008, Gardner et al. 2010) from surveys using unstructured spatial sampling (Russell et al. 2012, Proffitt et al. 2015). Estimating cougar abundance in this fashion requires a high amount of effort or auxiliary data (i.e., collar data; Paterson et al. 2019). The intensive effort required for both census and genetic SCR techniques reduces their utility for broad-scale monitoring. Attempts to measure cougar populations with remote cameras have had varied success. When a portion of the population can be identified, such as tropical populations in which individuals have heavy scarring, mark-resight models can be used (Rich et al. 2014). Individual cougars in Rocky Mountain populations in North America cannot be reliably identified (Alexander and Gese 2018), and the unmarked, spatial count model performs poorly without auxiliary information, such as collar data (J. S. Ruprecht, Oregon State University, unpublished data). The time- and space-to-event models do not require individual identification or auxiliary data and scale well to larger study areas compared to methods that require intensive effort; however, the low encounter rates of low-density populations could limit the efficiency of the time- and space-to-event models.

Our objective was to compare estimates of cougar abundance obtained using the time- and space-to-event models to concurrent estimates based on genetic SCR to test the applicability and efficacy of the time- and space-to-event models for species that live at low densities. We also estimated cougar abundance using the random encounter model (REM; Rowcliffe et al. 2008), another method for estimating abundance from encounter rates with cameras that has been used to estimate the abundance of African lions (*Panthera leo*; Cusack et al. 2015) to compare the space- and time-to-event models to an alternative camera-based approach.

STUDY AREA

We sampled 2 study areas in Idaho, USA (Fig. 1) over 3 winters (2016–2019). Both study areas were classified as ungulate winter range by Idaho Department of Fish and Game (IDFG). The first study area (~700 km²) was located in Boise National Forest in central Idaho along the Middle and South forks of the Payette River. Elevation ranged from 850 m to 2,460 m. The area received 65.6 cm of annual precipitation, concentrated in the winter. Average winter snow cover (Nov–Mar) was 30.5 cm at 1,200 m. Average winter temperature was -1.7°C , and average summer temperature (Apr–Oct) was 12.6°C . The predominant vegetation type was mixed conifer forest. Undeveloped forest occupied most of the study area, but some residential and agricultural development was present at lower elevations. The dominant prey species were elk (*Cervus canadensis*) and mule deer (*Odocoileus hemionus*), and the other large carnivores present were wolves (*Canis lupus*), black bears (*Ursus americanus*), and coyotes (*C. latrans*).

The second study area (~900 km²) was in southeastern Idaho along the western front of the Bear River Range and was sampled for 2 winters (2017–2019). Elevation ranged from 400 m to 2,700 m. The area received 32.0 cm of annual



Figure 1. Idaho, USA, with the central (left) and southeastern (bottom right) field sites for cougar camera surveys (2017–2019) in black with Esri World Hillshade Base Map depicting topography.

precipitation with a spike in the spring and lull in the summer. The average winter temperature was -1.2°C and average summer temperature was 14.5°C . At higher elevations, mixed coniferous forest was the dominant vegetation type, at lower elevations, sage brush (*Artemisia* spp.) steppe and juniper (*Juniperus scopulorum*) dominated. The western edge of the study area extended into the Cache Valley, which was dominated by agricultural fields. The dominant prey species was mule deer, and black bears and coyotes made up the rest of the large carnivore community. Wolves were absent.

METHODS

Field Methods

At both field sites, we overlaid a grid of 10-km^2 cells on ungulate winter range (Fig. 2) to define the study area. In the central Idaho site, we defined the grid using elk winter range. In the southeastern Idaho site, we defined the grid using a combination of elk and mule deer winter range. We targeted ungulate winter range as a proxy for cougar winter range, assuming that cougars follow the primary prey populations (Stoner et al. 2018). Ungulate winter range generally favored south-facing slopes, low elevations, and riparian areas (Bergen et al. 2016). We used the same grid for the camera and genetic sampling. The 10-km^2 cell size ensured that individuals would be available to be detected in multiple cells, which is an assumption of SCR models but does not matter for space- or time-to-event models or REM. We surveyed the central Idaho site during winters 2016–2017, 2017–2018, and 2018–2019 and surveyed the southeastern Idaho site in 2017–2018 and 2018–2019.

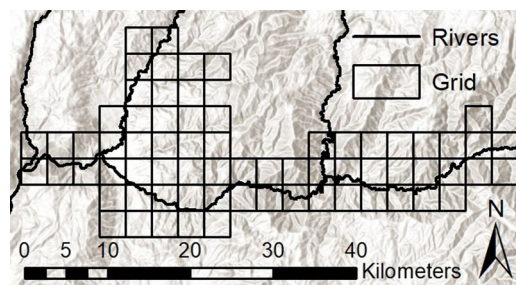


Figure 2. The central Idaho, USA, field site showing local relief (Esri World Hillshade Base Map) and the grid used for genetic and camera sampling of cougars, 2017–2019. Each grid cell is 10km^2 . The extent of the grid was defined by predicted ungulate winter range.

Staff from IDFG set up and maintained motion-sensitive camera grids. They identified 2–3 potential camera sites for each cell based on riparian areas and predicted cougar travel corridors (Blake and Gese 2016) within the ungulate winter range. Field crews selected 1 camera site at which to deploy a camera in each cell based on ease of access. At the site, crews placed cameras approximately 3 m high in trees to prevent theft and pointed cameras down to ensure drifting snow did not cover the cameras. They placed cameras overlooking roads or game trails whenever possible. We developed the camera placement protocol with occupancy and SCR models in mind, so it did not follow strict random sampling protocols. Field crews measured the width of each viewshed as the distance along the trail through which the camera triggered during walk tests. We took more extensive measurements of viewsheds *ex situ* to measure the area and cross sections of the viewsheds (Supporting Information). Crews deployed cameras in September and October of each year and retrieved them in April and May of the following year with no visits through the winter. We used only pictures from 1 November through 31 March to limit inference to density on winter range.

Field crews collected genetic samples from backtracking, harvest, and biopsy darting using hounds to tree cougars between December and March of each winter (Russell et al. 2012, Beausoleil et al. 2016). The backtracking and biopsy darting crews used unstructured spatial sampling to search for cougar tracks (Russell et al. 2012, Proffitt et al. 2015). Once they found a track, crews either backtracked it to search for hair and scat or followed it using hounds to tree the cougar. Rather than dividing effort equally among cells, search could adapt to access, snow availability, and presence of cougar tracks. Crews recorded distance searched for each cell using global positioning system (GPS) track logs to account for variable effort between cells. Field crews conducted biopsy darting during the first year of sampling in central Idaho (2016–2017) but then restricted darting to southeastern Idaho in 2017–2018 and 2018–2019. Crews collected data following an approved University of Montana Institutional Animal Care and Use Committee protocol (016-17HRWB-041117).

Models

We used a movement speed estimate of 8.9 km traveled per day (K. A. Zeller, Aldo Leopold Wilderness Research

Institute, unpublished data) and the mean of the viewshed widths (5.8 m) to define the time-to-event sampling period as 56.3 seconds. Zeller estimated the movement speed naively from distance moved divided by time using 5-minute fix intervals based on movement data from 6 female and 4 male cougars that were GPS-collared in the Santa Ana Mountains of southern California, USA (Zeller et al. 2016). We explored the effect of differing movement speed on our population estimate (see below). We defined an occasion for the time-to-event model as 500 periods. The choice of occasion length is arbitrary and should not have an effect on the final estimate. For each occasion, we recorded the number of periods that passed before a cougar appeared (TTE) at each camera. After 500 periods, we right censored the measured TTE, meaning it took longer than 500 periods for a cougar to appear, and started a new occasion. We estimated density in cougars per camera viewshed with equation 1. For the final reported density, we converted density to cougars/100 km² using an estimate of 45 m² (Supporting Information) for viewshed area. For the space-to-event model, we estimated density using equation 2. Occasions for the space-to-event model were spaced at 5-minute intervals (e.g., 0100, 0105, 0110). The cameras took only motion-trigger pictures, rather than motion-trigger and timed pictures. Because pictures are unlikely to be taken at precise times (down to the second), we included cougars as detected if they appeared on camera within 30 seconds of each occasion. We right censored data if a cougar did not appear on any camera during a given occasion, meaning that more space would need to be sampled to observe a cougar than is covered by the sum of all camera viewsheds. For both models, we estimated λ using log-likelihood, and calculated 95% confidence intervals as $\hat{\lambda} \pm (\text{SE} \times 1.96)$.

The REM estimates density directly from detection rate using

$$\text{Density} = y/tvd, \quad (3)$$

where y is the number of detections, t is the time period, v is the average movement speed of the population, and d is the average length of viewshed from every angle of approach (Supporting Information; Rowcliffe et al. 2008). We used the same movement speed estimate as before (8.9 km/day) and estimated d as 6.46 m. We estimated variance through bootstrapping by camera. We did not include variance caused by variation in the size of viewsheds or animal movement speed, which can both be incorporated into the model (Rowcliffe et al. 2008).

For the time- and space-to-event models and the REM, we specified all of the variables *a priori* and report the resulting estimates. We conducted *post hoc* analyses to examine the effects of using alternative values for the variables (e.g., animal movement speed and length of occasions). We ran the time-to-event model and REM with movement speeds 50% higher and lower than the original movement speed (4.45 km/day and 13.35 km/day). We also ran the time-to-event model with 100 periods and 1,000 periods per

occasion. For the space-to-event model, we tested 3 amounts of time between occasions (1, 3, and 5 min) and 4 buffers around the snapshots in time (5, 10, 15, and 30 seconds). We also looked at the effect of using more or fewer cameras on the space- and time-to-event models by resampling the data to 25, 50, 100, 200, and 500 cameras. We ran each resample for 1,000 iterations. To resample the time-to-event data, we selected cameras, with replacement, up to the target number. Resampling the space-to-event data follows a similar procedure but also requires randomizing the timing of detections within cameras. If camera C had a detection at 1200 and was selected in the resampling 3 times, that detection would be assigned, randomly, to 3 times rather than all timing of detections being kept at 1200. For all of the *post hoc* analyses, we focused on a single survey, the 2017 survey in central Idaho. We chose the central Idaho 2017 survey because it had one of the lowest encounter rates and the lowest number of non-right censored STE occasions, making it the most representative for sampling a low-density population.

For the SCR density estimates, we assigned each observation to a hypothetical trap at the center of the cell in which the observation occurred. We modeled the probability of observing individual i at trap j (p_{ij}) as

$$p_{ij} = p_{0j} \times g_{ij}, \quad (4)$$

where p_{0j} is the probability of observing a cougar with a center of activity at the location of hypothetical trap j , and g_{ij} is the effect of distance between the activity center and trap location (Proffitt et al. 2015). We modeled g_{ij} as a half normal decay function with

$$g_{ij} = \exp(-d_{ij}/2\sigma^2), \quad (5)$$

where d_{ij} is the distance between the activity center of animal i and trap j , and σ describes the rate at which detections decline as distance from the activity center increases (Gardner et al. 2010, Russell et al. 2012). We used 2 models for p_{0j} , one where it is held constant across cells, and one where it varies based on the amount of search effort in cell j according to the generalized linear model

$$\text{logit}(p_{0j}) = B_0 + B_1 \times \text{Effort}_j, \quad (6)$$

where Effort_j is the centered and scaled distance searched in cell j (Russell et al. 2012, Proffitt et al. 2015).

We fit the SCR model in a Bayesian framework using JAGS (Plummer 2017) implemented through R (R Core Team 2019) with the rjags (Plummer et al. 2019) package. We augmented the observed encounter histories with 1,000 all-zero encounter histories. We assigned each encounter history as belonging to a real or imaginary animal, and estimated abundance as the number of real animals. We buffered the camera grid by 10 km in every direction and used a random uniform distribution within that buffered zone as the prior for activity centers. We used a diffuse normal distribution for the priors on B_0 and B_1 and a diffuse half normal distribution from zero to infinity as the prior for σ .

We ran each model for 5,000 iterations in the adaptation phase, discarded the next 20,000 iterations as burn-in, and kept 75,000 iterations, thinned by 10, as the posterior distribution.

We evaluated goodness of fit for the SCR models using 2 Bayesian P -values (Gelman and Rubin 1992), 1 for the encounter process and 1 for the spatial point process (Russell et al. 2012, Proffitt et al. 2015). For the encounter process, we compared the discrepancy measures of the observed encounter rate and an encounter rate simulated from the posterior distribution using

$$D = \sum_{i=1}^N (\sqrt{n_i} - \sqrt{e_i})^2, \quad (7)$$

where D is the discrepancy measure, N is the total number of individuals, n_i is encounter frequency (observed or simulated) of individual i , and e_i is the expected encounter frequency of individual i under the model. The Bayesian P -value for the encounter process is the proportion of steps in the Markov chain Monte Carlo where $D(\text{observed})$ is greater than $D(\text{simulated})$. For the goodness-of-fit test for the spatial point process, we used

$$I = (G - 1) \times s^2 / \bar{n}, \quad (8)$$

where G is the number of grid cells, \bar{n} is the average number of activity centers per grid cell, and s is the variance of activity centers in each grid cell. To calculate the Bayesian P -value, we compared I calculated from the posterior distribution and I calculated from simulations of spatial randomness. The P -value is the proportion of times that I (posterior) is greater than $I(\text{simulated})$. For both Bayesian P -values, values near 0.5 indicate good fit, and values near 0 or 1 indicate poor fit. Code to run the analyses presented here is available in a public repository on Kenneth Loonam's GitHub (<https://github.com/keloonam>).

RESULTS

Camera-Based Methods

The number of cameras functional for some portion of each survey varied among sites and years (Table 1) from a high of 77 cameras functional for a portion of the southeastern

Table 1. The variation in camera effort among 5 surveys of cougar populations, Idaho, USA. Cameras represents the number of cameras that were functional for at least a portion of the survey. We also present the number of observations that were not right censored (a cougar appeared on camera) for the time-to-event (TTE) and space-to-event (STE) analyses. There were 43,489 observations in each survey for the space-to-event model (the number of 5-min intervals in the study period) and approximately 35,000 observations for the time-to-event model (the exact number depends on the number of cameras functional during each occasion).

Site	Year	Cameras	TTE	STE
Central ID	2017	70	45	7
Central ID	2018	67	81	17
Central ID	2019	64	74	26
Southeast ID	2018	77	53	11
Southeast ID	2019	71	40	9

Idaho 2018 survey, to a low of 64 cameras for the central Idaho 2019 survey. The number of occasions during which a cougar was observed for the space-to-event and time-to-event analyses also varied among surveys (Table 1).

Estimates of density from the 2 camera-based models varied between years in the central Idaho site and between models for the 2019 survey of the central Idaho site (Fig. 3). In 2017, density in the central Idaho site was estimated at 6.26 (95% CI = 4.43–8.10) cougars/100 km² by the time-to-event model, 5.07 (95% CI = 1.30–8.85) cougars/100 km² by the space-to-event model, and 6.91 (95% CI = 3.89–9.94) cougars/100 km² by the REM. In 2019 the estimates were notably higher and diverged from each other, with the time-to-event model estimating 12.13 (95% CI = 9.41–14.86) cougars/100 km², the space-to-event-model estimating 20.24 (95% CI = 12.48–28.00) cougars/100 km², and the REM estimating 14.29 (95% CI = 4.91–23.68) cougars/100 km². Estimates of density in the southeastern Idaho site were more consistent. In 2018, the time-to-event, space-to-event, and REM models estimated 6.88 (95% CI = 5.03–8.72), 7.33 (95% CI = 3.01–11.66), and 9.19 (95% CI = 5.97–13.84) cougars/100 km², respectively. The estimates of density remained similar in 2019 with the time-to-event, space to event, and REM models estimating 6.20 (95% CI = 4.26–8.15), 6.19 (95% CI = 2.14–10.25), and 6.98 (95% CI = 3.74–10.23) cougars/100 km², respectively.

In our *post hoc* analyses, the time-to-event model was not affected by changing the number of periods in each occasion (Fig. 4A). Both the time-to-event model and the REM were sensitive to the speed estimate used. When we used a speed estimate 50% lower, the time-to-event and REM estimates of density both doubled (Fig. 4B). When we increased the speed estimate by 50%, the estimates of density from both models fell by 33%. In the space-to-event model, changing the buffer time period had a large effect on the estimate of density, with the highest estimates from the 30-second buffer (5.07, 4.36, and 8.24 cougars/100 km², from the 5-min, 3-min, and 1-min wait times, respectively), and the lowest estimates coming from the 5-second buffer (0.43 and 1.00 cougars/100 km² from the 3-min and 1-min wait times; Fig. 4C). No cougar pictures were taken within 5 seconds of a 5-minute interval in the central Idaho 2017 survey, so there was no estimate of density for the 5-minute wait time with a 5-second buffer. In the resampling analysis to look at the effect of using more or fewer cameras, the point estimates of density from the 1,000 runs of each scenario were normally distributed with means equal to the estimated density from the original survey, as expected with bootstrapping techniques. The standard deviation of the estimates decreased as the number of cameras increased. For the time-to-event model, the standard deviation of the estimates was 2.92 cougars/100 km² at 25 cameras and 0.55 cougars/100 km² at 500 cameras. The space-to-event model was slightly less precise with standard deviations of 3.57 and 0.80 cougars/100 km² at 25 and 500 cameras, respectively. The space-to-event model also failed to estimate density in 109 of the 25 camera resamples, 21 of the 50 camera resamples, and 1 of the 100 camera resamples because no cameras with detections were sampled. We

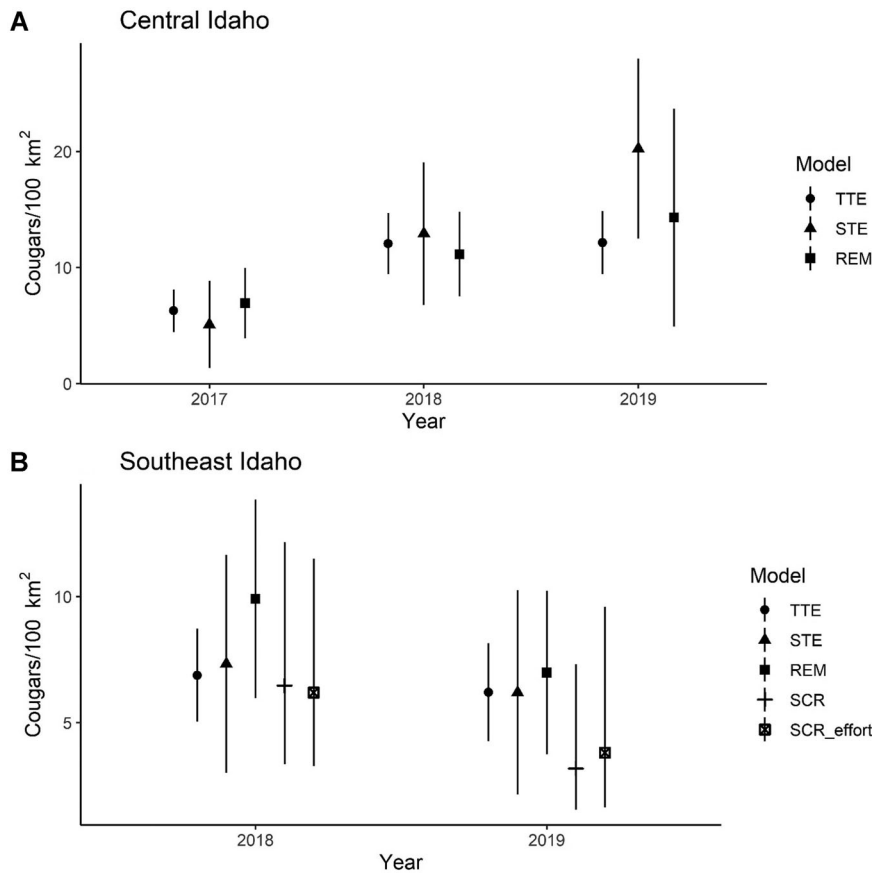


Figure 3. A) Estimates of cougar density and 95% confidence intervals from the space-to-event (STE) and time-to-event (TTE) camera models from the 3 surveys in the central Idaho, USA, field site. B) Cougar density estimates from the space-to-event and time-to-event models, random encounter models (REM), genetic spatial capture recapture (SCR) models, and SCR models considering search effort from the 2 surveys in the southeast Idaho site. Intervals shown are 95% confidence intervals for the space- and time-to-event models and 95% credible intervals for the SCR models.

recorded these as estimates of 0 cougars/100 km² when reporting the mean and standard deviations of the estimates.

DNA-Based SCR

The number of individuals detected in the genetic sampling and the recapture rates (the average number of detections per individual) varied across surveys and were generally lower in the central Idaho site where biopsy darting was restricted to 2017. At the central Idaho site, we detected 21, 16, and 6 individuals with recapture rates of 1.19 (1 individual captured in a single cell and 1 captured in 2 cells), 1, and 1 in 2017, 2018, and 2019, respectively. A recapture rate of 1 indicates that no individuals were detected multiple times. At the southeastern Idaho site, we detected 32 and 18 individuals with recapture rates of 1.38 (6 individuals captured in 2 cells, and 2 captured in 2 cells) and 1.22 (1 individual captured in 2 cells and 2 captured in 3 cells) in 2018 and 2019, respectively.

Recapture rates of 1 do not contain any information for capture recapture models, and the central Idaho 2017 model failed to converge. Density estimates from the genetic sampling are restricted to the southeastern Idaho site. Including effort per grid cell in estimating cell-specific detection probabilities did not change the estimates of density within years, but there was variation in the estimates between years (Fig. 3). The SCR model estimated 6.47 (95%

CRI = 3.35–12.15) cougars/100 km² in the southeastern Idaho site in 2018, the year with the best recapture rate, and 3.17 (95% CRI = 1.55–7.31) cougars/100 km² in 2019. The null model fit the data well for both the encounter process and point process in both years, but including effort in estimating detection probability reduced the model fit for the encounter process, despite the effort covariate appearing significant (Table 2).

DISCUSSION

Combining the efficiency of observing animals through remote cameras with the time-to-event approach allows the estimation of low-density populations without the need for individual identification. The methods are general enough to apply to many different species, with the low-density species tested here representing a difficult case. In this difficult case, even biased camera sampling (i.e., non-random placement) resulted in performance comparable to existing, intensive efforts. With randomly placed cameras and sufficient effort, these methods should provide reliable estimates of low-density populations, making them a viable option for monitoring a diverse array of species.

In the southeastern Idaho site, the estimates of density from both models were consistent with each other and the SCR estimates (Fig. 3). The estimates from the

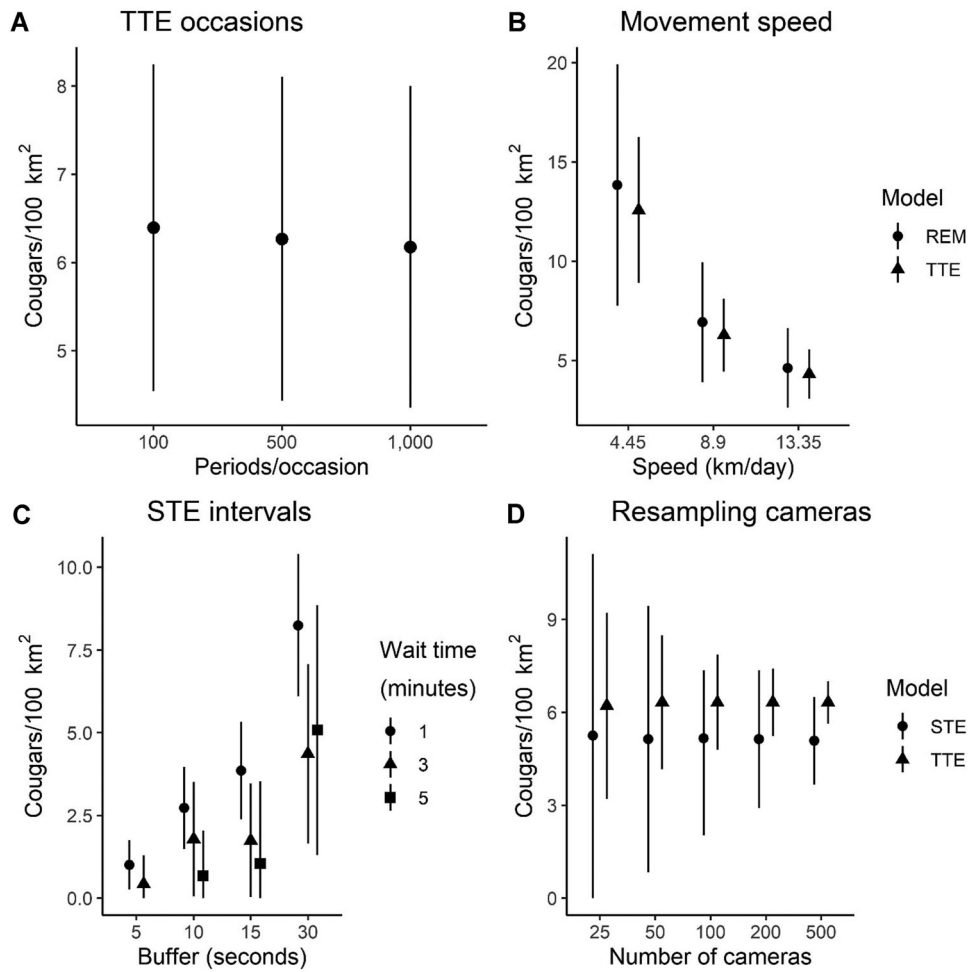


Figure 4. Estimates of cougar density from *post hoc* analyses of the central Idaho, USA, survey, 2017. A) Estimates of cougar density and 95% confidence intervals from the time-to-event (TTE) model using 3 different lengths for occasions: 100, 500, and 1,000 periods. B) Estimates of cougar density and associated 95% confidence intervals from the TTE model (triangles) and random encounter model (REM; circles) using the original movement speed (8.9 km/day), 50% decreased movement speed (4.45 km/day), and 50% increased movement speed (13.35 km/day). C) Estimates of cougar density and 95% confidence intervals using the space-to-event (STE) model with 3 different wait times between occasions and 3 different buffer periods. The wait times of 1, 3, and 5 minutes define the amount of time between samples, which are points in time. The buffer defines the length of time, on either side of a sample, in which cougars were included as detected for the occasion. With a wait time of 5 minutes and a 30-second buffer, cougars were included if they appeared on camera between 0159:30 and 0200:30 for the first occasion then between 0204:30 and 0205:30 for the next occasion. D) The means of estimates of density from resampling cameras, with replacement, and estimating density on the new data set with the time-to-event (triangle) and space-to-event (circle) models. We ran each scenario resampling the data to a different number of cameras (25, 50, 100, 200, and 500) 1,000 times. The confidence intervals shown are the mean of the upper and lower limits of the confidence intervals from each run.

Table 2. Results from genetic spatial capture recapture models used to estimate cougar density across 2 surveys of a field site in southeastern Idaho, USA. The model column indicates whether search effort within cells was included as affecting cell-specific detection probability ($B_0 + B_1 \text{Effort}$) or not (B_0). Density is the estimated number of cougars per 100 km². B_{Effort} is the estimate of the effect of centered and scaled search effort on detection probability. Sigma estimates the effect of distance between individual activity centers and cell centers on detection probability. Encounter and point process values are Bayesian P -values representing how well the data fit the model. Values in parentheses are the 95% credible intervals.

Year	Model	Density (cougars/100 km ²)	B_{Effort}	Sigma	Encounter	Point process
2018	B_0	6.47 (3.35–12.15)		3.49 (2.36–5.63)	0.36	0.52
2018	$B_0 + B_1 \text{Effort}$	6.19 (3.26–11.50)	0.50 (0.16–0.91)	3.50 (2.32–5.61)	1.00	0.55
2019	B_0	3.17 (1.55–7.31)		1.67 (1.14–2.97)	0.53	0.28
2019	$B_0 + B_1 \text{Effort}$	3.81 (1.63–9.59)	2.20 (–0.63–9.01)	1.73 (1.13–3.33)	1.00	0.29

time-to-event model were more precise than the SCR estimates. These estimates from the southeastern Idaho site and the first year survey of the central Idaho site also compared well to estimates in the literature of cougar density in the Northern Rockies from genetic SCR, which have ranged from 3.2 ± 0.5 (SD) to 6.7 ± 3.1 (Russell et al. 2012, Proffitt et al. 2015); the estimates of density were within the range of reported values and comparably precise. In 2018 and 2019, the estimates from the central Idaho site diverged from values in the literature and from each other, potentially because of camera placement and small sample sizes. Throughout the study, the time-to-event model was more precise than the REM or space-to-event. The time and space-to-event models assume that animals are Poisson distributed at the scale of viewsheds, allowing them to be more precise than REM. The REM and time-to-event model incorporate animal movement, increasing precision compared to space-to-event, which does not require a measurement of movement speed (Gilbert et al. 2020). The precision of REM was also more variable than time- or space-to-event. The REM measures variance by bootstrapping across cameras. If detections are concentrated at a few cameras, the REM will be less precise.

The time and space-to-event models and REM are sensitive to camera placement, which, in this study, was non-random at 3 separate scales. First, we defined the study area by ungulate winter range, which we used as a proxy for cougar winter range. Second, within each grid cell, we selected camera locations based on predicted cougar movement corridors during winter. Finally, at the selected locations, crews placed cameras on roads and trails whenever available. Estimating density on winter range allowed the estimates to be compared to the SCR estimates and to values in the literature of cougar density in the Northern Rockies, which have traditionally been restricted to winter range (Hornocker 1969, Seidensticker et al. 1973, Russell et al. 2012, Proffitt et al. 2015), but may have contributed to variation in estimates between years. If density on winter range varies with winter conditions, potentially because prey movement onto and off of winter range depends on the timing or depth of snow, and cougars follow the prey, encounter rates with cameras targeting winter range will also vary. In that case, between-year variation in conditions, such as snowfall, would cause variation in the density estimates between years. Non-random placement at fine scales (i.e., targeting predicted travel routes) could have increased detection rates and biased the estimates high regardless of winter conditions, which may have contributed to the estimates of density for the central Idaho site in 2018 and 2019 being higher than the values in the literature for cougar density. Completely random camera placement can be daunting with low-density populations given the possibility of low or no detections; however, if non-random camera placement in this study did increase detections and thus bias the estimates of density high, the observed detection rates are equivalent to the expected detection rates of populations living at the estimated densities ($6\text{--}12$ cougars/ 100 km^2 for time-to-event and $5\text{--}20$ cougars/ 100 km^2 for space-to-event)

given random camera placement. Given that, the effort we used can be used as a starting point for understanding the effort necessary to sample other low-density species.

In practice, strict random sampling can be impractical. If a random point and angle have a camera facing into dense vegetation, that camera would not actually sample anything (the viewshed area would be 0 m^2) and would be excluded from the analysis. We recommend *a priori* rules for deploying cameras, such as a radius around a random or systematic point within which the camera can be placed freely. The size of that radius will depend on the study species and the landscape characteristics. As a general rule, if every camera overlooks a heavily used game trail near a limited resource, the radius is likely too large.

A few other factors could have contributed to variation in the estimates of cougar density, both in comparison to each other and to the literature. First, both the time-to-event and space-to-event models rely on an accurate measurement of the area sampled by the camera viewsheds (Moeller et al. 2018). We calculated viewshed area from *ex situ* measurements taken on cameras deployed to match the *in situ* measurements of viewshed width (Supporting Information). A more rigorous measurement of viewshed area *in situ*, for instance measuring trigger distance in multiple portions of the viewshed, could reduce a potential source of bias. If the area of the viewsheds is incorrect, the resulting bias will be linear. Equations 1 and 2 directly estimate density in animals per viewshed area, which is converted using the measured area. If the area is estimated to be 50 m^2 when in reality it is 25 m^2 , the estimated density will be biased low by 50%. Second, the time-to-event model relies on an accurate estimate of movement speed for the population (Moeller et al. 2018). We did not have data to estimate movement speed in the study areas, and therefore used an estimate from another cougar population that had fine-scale collar data (Zeller et al. 2016). If the movement speed of cougars varies significantly between populations, using that estimate could have biased our results. Overestimating movement speed will bias abundance estimates low and vice versa, as shown in the *post hoc* analysis of movement speed. An alternative to relying on estimates of movement speed from other populations would be to estimate movement speed directly from the camera data (Rowcliffe et al. 2014, 2016). Finally, the space-to-event model is sensitive to small sample sizes. The space-to-event model uses only the subset of detections that happen at a point in time for each occasion. In this study, the space-to-event time sample lasted 1 minute (30 seconds on either side of a point in time) and was taken every 5 minutes. Effectively, each cougar detection had a 1 in 5 chance of being used in the space-to-event model. At low sample sizes, random chance could have an outsized effect on the density estimate. This effect is reflected in the large confidence intervals of the space-to-event estimates and will be minimized as the number of cameras and animal density increase. In this study, the space-to-event sampling design influenced the divergence of the space-to-event and time-to-event estimates for the central Idaho site in 2019. The

length of the sample (1 min) may also have biased the space-to-event estimates high by including too many animals as detected during the snapshot. When relying on motion-triggered pictures for the space-to-event model, choosing the correct length for the window is a balancing act between accurately recording every animal that was in view at the time of the snapshot and potentially missing animals because a picture was not taken closely enough to the snapshot in time. We suggest using shorter sample lengths (e.g., 10 seconds) to more closely approximate a snapshot in time; however, time-lapse pictures should be used whenever possible (Moeller et al. 2018). With both time-lapse settings and motion-trigger settings, deploying more cameras will increase the number of occasions with detections.

The inconsistency of the genetic SCR estimates with sparse data was similar to that of the camera-based models. In 3 survey years, the SCR models could not be used because of a lack of recaptures despite high field effort. In the surveys that we could use, the SCR estimates varied between years at the same site and had large confidence intervals, similar to the space-to-event estimates. The SCR models with low sample sizes are sensitive to changes in individual capture histories, which likely influenced the variation in the estimates. Additionally, the SCR models with search effort included as a covariate failed the encounter process goodness-of-fit test despite the effort covariate appearing significant. Common sense dictates that search effort affects detection probability, and similar studies have found support for including search effort in the SCR model (Russell et al. 2012, Proffitt et al. 2015). The failure of the goodness-of-fit test with search effort included was likely due to insufficient recaptures. Given the effort required to recapture individuals of difficult to detect species, time- and space-to-event approaches may be more efficient than SCR in many scenarios.

Unlike camera arrays designed for occupancy or SCR analyses where cameras are placed to maximize detection probability, the time- and space-to-event models assume that animal movements are random in relation to camera placement (i.e., cameras are randomly located).

The SCR and capture-recapture methods more broadly rely on capturing the same individual multiple times, which can be difficult when capture probability is low. The individuals never detected do not contribute to the model. In contrast, in time- and space-to-event models, the occasions with no animal detected are almost as informative as the occasions with an animal detected. Occasions without detections are expected when surveying a population at low density. In fact, in 2019 we observed encounter frequencies as low as 40 out of approximately 35,000 occasions (Table 1), which resulted in a density estimate of approximately 5.5 individuals/100 km². The space- and time-to-event models work well with low encounter rates compared to capture-recapture techniques because the estimate of density depends as much on the ratio of occasions with detections to occasions without detections as it does on the observations (non-right censored occasions) of the time or space until an event occurs.

The time- and space-to-event models scale well compared to capture-recapture methods. Because SCR relies on capturing the same individual in multiple locations, it performs best when effort is concentrated in a small area. To survey a larger area, effort has to increase to keep the effort per unit area, and thus the probability of recaptures, consistent. The time- and space-to-event models do not rely on recapturing the same individual; they use only the encounter frequency of the study species across the entire study area. For this reason, a survey using 100 cameras would be as effective at estimating density in a large study area as it would in a small study area. Put differently, space-to-event and time-to-event methods sample the landscape, not the individuals in the population. The total number of cameras, not the density of cameras, determines precision. Care must still be taken to representatively sample the landscape, but a certain density of cameras is not required.

Camera-based estimators that scale to any size study area and effectively estimate the density of unmarked species could help address many of the issues with monitoring species such as cougars and make multi-species monitoring more feasible. Rare species and species that live at low densities typically require targeted effort during surveys, perhaps limiting the utility of a survey for sympatric species. A random sample of the study area will be random for every species, not just the target species, so using time- or space-to-event methods to monitor multiple species would only be reliant on all species of interest being detectable by the same camera setup.

MANAGEMENT IMPLICATIONS

The time-to-event and space-to-event models are effective tools for estimating abundance of unmarked populations. Even for species at low densities, and thus low encounter rates, the models perform well given enough cameras, in this case approximately 10,500 camera days. Estimating abundance of low-density, difficult to detect species using camera surveys, rather than intensive ground surveys or capture-recapture efforts, could make abundance estimates for those species more feasible and cheaper to obtain. With relatively efficient methods, point estimates of abundance could be used for management decisions more often or be obtained more frequently in conjunction with existing integrated population models or management plans such as those currently employed by some state agencies (Montana Fish Wildlife and Parks 2019).

ACKNOWLEDGMENTS

Any use of trade, firm, or product names is for descriptive purposes only and does not imply endorsement by the U.S. Government. K. A. Zeller generously reanalyzed data for us to provide the movement speed estimate used in both the time-to-event and random encounter models. M. P. Atwood, D. Dressel, E. Freeman, C. Hone, M. A. Hurley, Z. B. Lockyer, S. B. Roberts, N. Stohosky, J. L. Struthers, and J. Utz made this project possible. Field crews including E. L. Anderson, C. M. Argabright, D. A. Bernasconi, M. Danielson, J. Dougherty, J. Ellison, A. S. Emmel,

E. Fochtman, Z. Fogel, C. E. Jacobs, A. J. Koenig, J. M. Krohner, J. M. Labrie, K. J. Lamp, A. Nelson, J. M. Nelson, C. J. Peterson, A. Pisa, P. R. Rebholz, G. S. Robertson, P. Schirf, S. W. Servis, E. M. Shields, D. J. Thibodeau, W. Tropea, K. Wagner, B. Smith, and J. Johnson deployed the cameras and collected a phenomenal number of genetic samples. D. Noce, M. Sheu-Reyes, and P. Childers looked through hundreds of thousands of photos in search of cougars. Funding and support for this project were provided by IDFG, the Federal Aid in Wildlife Restoration Act, the Montana Cooperative Wildlife Research Unit, and the Wildlife Biology Program at the University of Montana.

LITERATURE CITED

- Alexander, P. D., and E. M. Gese. 2018. Identifying individual cougars (*Puma concolor*) in remote camera images—implications for population estimates. *Wildlife Research* 45:274–281.
- Beausoleil, R. A., J. D. Clark, and B. T. Maletzke. 2016. A long-term evaluation of biopsy darts and DNA to estimate cougar density: an agency-citizen science collaboration. *Wildlife Society Bulletin* 40: 583–592.
- Bergen, S., J. Horne, K. Anderson, and M. Hurley. 2016. Elk seasonal ranges in Idaho. Idaho Department of Fish and Game, Boise, USA.
- Blake, L. W., and E. M. Gese. 2016. Resource selection by cougars: Influence of behavioral state and season. *Journal of Wildlife Management* 80:1205–1217.
- Brochers, D. L., and M. Efford. 2008. Spatially explicit maximum likelihood methods for capture-recapture studies. *Biometrics* 64:377–385.
- Carbone, C., S. Christie, K. Conforti, T. Coulson, N. Franklin, J. R. Ginsberg, M. Griffiths, J. Holden, K. Kawanishi, M. Kinnaird, et al. 2001. The use of photographic rates to estimate densities of tigers and other cryptic mammals. *Animal Conservation* 4:75–79.
- Cusack, J. J., A. Swanson, T. Coulson, C. Packer, C. Carbone, A. J. Dickman, M. Kosmala, C. Lintott, and J. M. Rowcliffe. 2015. Applying a random encounter model to estimate lion density from camera traps in Serengeti National Park, Tanzania. *Journal of Wildlife Management* 79:1014–1021.
- Efford, M. 2004. Density estimation in live-trapping studies. *Oikos* 106:598–610.
- Gardner, B., J. A. Royle, M. T. Wegan, R. E. Rainbolt, and P. D. Curtis. 2010. Estimating black bear density using DNA data from hair snares. *Journal of Wildlife Management* 74:318–325.
- Gelman, A., and D. B. Rubin. 1992. Inference from iterative simulation using multiple sequences. *Statistical Science* 7:457–511.
- Gilbert, N., J. Clare, J. Stenglein, and B. Zuckerberg. 2020. Abundance estimation with camera traps. *Conservation Biology*. In press.
- Hornocker, M. G. 1969. Winter territoriality in mountain lions. *Journal of Wildlife Management* 33:457–464.
- Howe, E. J., S. T. Buckland, M. L. Després-Einspinner, and H. S. Kühl. 2017. Distance sampling with camera traps. *Methods in Ecology and Evolution* 8:1558–1565.
- Karanth, K. U. 1995. Estimating tiger *Panthera tigris* populations from camera-trap data using capture-recapture models. *Biological Conservation* 71:333–338.
- Karanth, K. U., and J. D. Nichols. 1998. Estimation of tiger densities in India using photographic captures and recaptures. *Ecology* 79: 2852–2862.
- Moeller, A. K., P. M. Lukacs, and J. S. Horne. 2018. Three novel methods to estimate abundance of unmarked animals using remote cameras. *Ecosphere* 9:e02331.
- O’Connell, A. F., J. D. Nichols, and K. U. Karanth. 2011. *Camera traps in animal ecology: methods and analyses*. Springer, New York, New York, USA.
- Paterson, J. T., K. Proffitt, B. Jimenez, J. Rotella, and R. Garrott. 2019. Simulation-based validation of spatial capture-recapture models: a case study using mountain lions. *PLoS ONE* 14:1–20.
- Plummer, M. 2017. JAGS: Just Another Gibbs Sampler. <mcmc-jags.sourceforge.net>. Accessed 12 Oct 2018.
- Plummer, M., A. Stukalov, and M. Denwood. 2019. Rjags. <<https://cran.r-project.org/web/packages/rjags/>>. Accessed 12 Oct 2018.
- Proffitt, K. M., J. G. Goldberg, M. Hebblewhite, R. Russell, B. Jimenez, H. S. Robinson, K. Pilgrim, and M. K. Schwartz. 2015. Integrating resource selection and harvest into spatial capture-recapture models for large carnivores. *Ecosphere* 6:1–15.
- R Core Team. 2019. R: a Language and Environment for Statistical Computing. R Foundation for Statistical Computing, Vienna, Austria.
- Rich, L. N., M. J. Kelly, R. Sollmann, A. J. Noss, L. Maffei, R. L. Arispe, A. Paviolo, C. D. De Angelo, Y. E. Di Blanco, and M. S. Di Bitetti. 2014. Comparing capture-recapture, mark-resight, and spatial mark-resight models for estimating puma densities via camera traps. *Journal of Mammalogy* 95:382–391.
- Rowcliffe, J. M., J. Field, S. T. Turvey, and C. Carbone. 2008. Estimating animal density using camera traps without the need for individual recognition. *Journal of Applied Ecology* 45:1228–1236.
- Rowcliffe, J. M., P. A. Jansen, R. Kays, B. Kranstauber, and C. Carbone. 2016. Wildlife speed cameras: measuring animal travel speed and day range using camera traps. *Remote Sensing in Ecology and Conservation* 2:84–94.
- Rowcliffe, J. M., R. Kays, B. Kranstauber, C. Carbone, and P. A. Jansen. 2014. Quantifying levels of animal activity using camera trap data. *Methods in Ecology and Evolution* 5:1170–1179.
- Royle, J. A., K. U. Karanth, A. M. Gopalaswamy, and N. S. Kumar. 2009. Bayesian inference in camera trapping studies for a class of spatial capture-recapture models. *Ecology* 90:3233–3244.
- Royle, J. A., and K. V. Young. 2008. A hierarchical model for spatial capture-recapture data. *Ecology* 89:2281–2289.
- Russell, R. E., J. A. Royle, R. DeSimone, M. K. Schwartz, V. L. Edwards, K. P. Pilgrim, and K. S. McKelvey. 2012. Estimating abundance of mountain lions from unstructured spatial sampling. *Journal of Wildlife Management* 76:1551–1561.
- Seidensticker, J. C., M. G. Hornocker, W. V. Wiles, and J. P. Messick. 1973. Mountain lion social organization in the Idaho Primitive Area. *Wildlife Monographs* 35:3–60.
- Stoner, D. C., J. O. Sexton, D. M. Choate, J. Nagol, H. H. Bernal, S. A. Sims, K. E. Ironside, K. M. Longshore, and T. C. Edwards. 2018. Climatically driven changes in primary production propagate through trophic levels. *Global Change Biology* 24:4453–4463.
- Zeller, K. A., K. McGarigal, S. A. Cushman, P. Beier, T. W. Vickers, and W. M. Boyce. 2016. Using step and path selection functions for estimating resistance to movement: pumas as a case study. *Landscape Ecology* 31:1319–1335.

Associate Editor: Ryan Long.

SUPPORTING INFORMATION

Additional supporting information may be found in the online version of this article at the publisher’s website.